Aerosol Science and Technology
Publication details, including instructions for authors and subscription information:
http://www.tandfonline.com/loi/uast20

Association of Airborne Virus Infectivity and Survivability with its Carrier Particle Size

Zhili Zuo [a], Thomas H. Kuehn [a], Harsha Verma [b], Sunil Kumar [b], Sagar M. Goyal [b], Jessica Appert [c], Peter C. Raynor [c], Song Ge [a] & David Y. H. Pui [a]

[a] Department of Mechanical Engineering, College of Science and Engineering, University of Minnesota, Minneapolis, Minnesota, USA

[b] Department of Veterinary Population Medicine, College of Veterinary Medicine, University of Minnesota, Saint Paul, Minnesota, USA

[c] Division of Environmental Health Sciences, School of Public Health, University of Minnesota, Minneapolis, Minnesota, USA

Accepted author version posted online: 06 Dec 2012.Published online: 27 Dec 2012.

To cite this article: Zhili Zuo, Thomas H. Kuehn, Harsha Verma, Sunil Kumar, Sagar M. Goyal, Jessica Appert, Peter C. Raynor, Song Ge & David Y. H. Pui (2013) Association of Airborne Virus Infectivity and Survivability with its Carrier Particle Size, Aerosol Science and Technology, 47:4, 373-382, DOI: 10.1080/02786826.2012.754841

To link to this article: http://dx.doi.org/10.1080/02786826.2012.754841

Aerosol Science and Technology, 47:373–382, 2013

ISSN: 0278-6826 print / 1521-7388 online
DOI: 10.1080/02786826.2012.754841

Association of Airborne Virus Infectivity and Survivability with its Carrier Particle Size

Zhili Zuo,[1] Thomas H. Kuehn,[1] Harsha Verma,[2] Sunil Kumar,[2] Sagar M. Goyal,[2] Jessica Appert,[3] Peter C. Raynor,[3] Song Ge,[1] and David Y. H. Pui[1]

[1]*Department of Mechanical Engineering, College of Science and Engineering, University of Minnesota, Minneapolis, Minnesota, USA*
[2]*Department of Veterinary Population Medicine, College of Veterinary Medicine, University of Minnesota, Saint Paul, Minnesota, USA*
[3]*Division of Environmental Health Sciences, School of Public Health, University of Minnesota, Minneapolis, Minnesota, USA*

Although laboratory generated virus aerosols have been widely studied in terms of infectivity and survivability, how they are related to particle size, especially in the submicron size range, is little understood. Four viruses (MS2 bacteriophage, transmissible gastroenteritis virus, swine influenza virus, and avian influenza virus) were aerosolized, size classified (100–450 nm) using a differential mobility analyzer (DMA), and collected onto gelatin filters. Uranine dye was also nebulized with the virus, serving as a particle tracer. Virus infectivity assay and quantitative reverse transcription-polymerase chain reaction were then used to quantify the amount of infectious virus and total virus present in the samples, respectively. The virus distribution was found to be better represented by the particle volume distribution rather than the particle number distribution. The capacity for a particle to carry virus increased with the particle size and the relationship could be described by a power law. Virus survivability was dependent on virus type and particle size. Survivability of the three animal viruses at large particle size (300–450 nm) was significantly higher than at particle size close to the size of the virion (100–200 nm), which could be due to the shielding effect. The data suggest that particle size plays an important role in infectivity and survivability of airborne viruses and may, therefore, have an impact on the airborne transmission of viral illness and disease. The data in this study do not support the use of MS2 bacteriophage as a general surrogate for animal and human viruses.

Received 29 August 2012; accepted 21 November 2012.
This study was supported by a grant from CDC-NIOSH (SR01OH009288-03) and the Center for Filtration Research at the University of Minnesota. The ideas presented are solely the responsibility of the authors and do not necessarily represent the official views of CDC-NIOSH.
Address correspondence to Zhili Zhou, Department of Mechanical Engineering, College of Science and Engineering, University of Minnesota, 111 Church Street SE, Minneapolis, MN 55455, USA. E-mail: zuoxx011@umn.edu

[Supplementary materials are available for this article. Go to the publisher's online edition of *Aerosol Science and Technology* to view the free supplementary files.]

1. INTRODUCTION

The world-wide outbreaks of coronavirus-caused severe acute respiratory syndrome (SARS), H5N1 bird flu, and H1N1 novel influenza have caused substantial health impact and have increased public concerns for the spread of viral diseases. Respiratory viruses such as influenza virus are traditionally believed to be transmitted by direct contact, indirect contact with fomites, and large-sized droplets. However, recent human subject studies and field measurements have suggested that the aerosol route could also be an important mode of virus transmission (Sattar and Ijaz 1987; Fabian et al. 2008; Tellier 2009).

For aerosol transmission to occur, a particle must carry infectious virus and the virus in the carrier particle must survive (remain infectious) in air before it reaches a susceptible host to initiate infection. In general, airborne infectious virus is difficult to recover due to its extremely low concentration in air and because of inadequacy of currently used air samplers. The behavior of artificially generated virus-carrying particles and their survival have been studied under laboratory conditions since the 1930s. It has been found that airborne influenza virus and coronavirus survive better at low RH and low ambient temperature (Hemmes et al. 1960; Harper 1961; Schaffer et al. 1976; Ijaz et al. 1985; 1987; Kim et al. 2007).

However, most of the laboratory studies mentioned above used sampling instruments such as liquid impingers that provide little information on particle size of the collected virus aerosol, which has been identified to be one of the most important factors affecting airborne transmission (Morawska 2006; Gralton et al. 2011). Particle size governs the transport of virus aerosol, its deposition in the human respiratory tract, as well as its control by

filtration (Eninger et al. 2008; Zuo et al. 2012). Particle size may also play a role in the minimum infectious dose of a given virus. For instance, small-sized aerosol inhalation of human influenza virus and adenovirus yielded a much lower median infectious dose than intranasal inoculation with droplets of much larger size (Alford et al. 1966; Hamory et al. 1972; Douglas 1975). In an exposure study using a murine model (Scott and Sydiskis 1976), airborne influenza virus of small particle size (2 μm) resulted in a lower infectious dose than the larger-sized particles (10 μm). Therefore, it is not sufficient to measure only particle size-integrated infectivity/survivability of airborne virus.

To better understand virus transmission by aerosols, it is important to determine the relationship between airborne virus infectivity/survivability and particle size (Gralton et al. 2011). Only a few studies are available on this issue in the scientific literature. To determine the distribution of infectious virus among polydisperse particles, an Andersen cascade impactor was used to sample aerosols of coxsackie virus A-21 (Gerone et al. 1966) and simian rotavirus (Ijaz et al. 1987). The concentration of infectious virus appeared to be related to particle volume distribution for particle size >0.5 μm. Using the same instrument, Appert et al. (2012) confirmed the above findings for MS-2 bacteriophage, but not for adenovirus. Tyrrell (1967) found that rhinovirus survived better in coarse particles (>4 μm) than in smaller particles (0–4 μm), while adenovirus infectivity was best preserved in the size range of 0.56–1.9 μm compared with 1.9–10 μm (Appert et al. 2012), indicating that particle size may also affect virus survivability.

Although the use of size-segregated samplers, such as impactors, provides size fractionation for virus infectivity, not much is known about virus aerosol particles of <0.5 μm, the size of most human respiratory particles (Haslbeck et al. 2010; Holmgren et al. 2010), probably because of the large cut size and low size resolution of impactors. To extend the understanding on submicron particles, Hogan et al. (2005) used a differential mobility analyzer (DMA) in combination with a liquid impinger to collect size-classified MS2 and T3 bacteriophage aerosol particles. The virus distribution and particle number distribution were found to be different. Lee (2009) later applied the same sampling approach for MS2 and showed that both virus infectivity and survivability increased with particle size. Nevertheless, both studies used bacteriophages and how well the results of bacteriophages represent those of human and animal viruses remains an issue (Appert et al. 2012).

The objective of this study was to examine infectivity and survivability of three airborne animal viruses as a function of their carrier particle size in the submicron size range using a newly developed sampling method. In addition, the behavior of widely used MS2 bacteriophage was studied for comparative purposes.

2. MATERIALS AND METHODS

2.1. Propagation and Titration of MS2 Bacteriophage

MS2 bacteriophage (ATCC 15597-B1) is a small (27–34 nm), icosahedral, non-enveloped, single stranded, positive sense RNA virus, infecting only the male *Escherichia coli* (those bearing an F pilus) (Valegard et al. 1990). For the purposes of this study, we considered MS2 as a model virus because it has been widely used in many virus aerosol studies (Eninger et al. 2008; Lee 2009; Appert et al. 2012). The virus was propagated in *E. coli* famp (ATCC 700891), as described elsewhere (Appert et al. 2012). Briefly, 0.1 mL of MS2 and 1 mL of a log phase culture of *E. coli* were added to top agar tubes held at 48°C. After mixing, the contents of the tubes were poured on trypticase soy agar (TSA) plates. The top agar was allowed to solidify followed by inversion and incubation of plates at 37°C for 24 h. After plaques were confluent (within 24 h of incubation), 5 mL of tryptic soy broth (TSB) was added to each plate. After 2 h at room temperature, the solution was aspirated, centrifuged at 2500 × g for 15 min, and sterile-filtered. The resulting bacteriophage stock was aliquoted into 50 mL tubes, followed by storage at −80°C until use. The amount of MS2 bacteriophage in virus stock and various other samples was determined by using a double agar layer procedure as described elsewhere (Appert et al. 2012). The amount of virus was expressed as plaque forming units per unit volume of the sample (PFU/mL).

2.2. Propagation and Titration of Animal Viruses

Three animal viruses were used, e.g., transmissible gastroenteritis virus (TGEV; Purdue strain) of pigs, avian influenza virus (AIV; A/chicken/Maryland/2007[H9N9]), and swine influenza virus (SIV; A/swine/Minnesota/2010 [H3N2]). The TGEV, a member of *Coronaviridae*, is spherical (100–150 nm), enveloped, single stranded, positive sense RNA virus, causing gastrointestinal infections in pigs (Tajima 1970). Influenza viruses are also spherical (80–120 nm), contain eight segments of single-stranded RNA, and cause respiratory disease in pigs, poultry, and other animal species (Lamb and Choppin 1983). The three animal viruses share physical and genetic similarity to human viruses (Lamb and Choppin 1983; Jackwood 2006) and were, therefore, used as surrogates for human SARS virus and influenza virus.

The TGEV was propagated in swine testicular (ST) cells, while the two influenza viruses were propagated in Madin–Darby canine kidney (MDCK; ATCC CCL-34) cells. The cells were grown in Minimum Essential Medium (MEM) with Earle's salts supplemented with L-glutamine, (Mediatech, Inc., Herndon, VA, USA), 8% fetal bovine serum (FBS; Gibco, Life Technologies, Corp., NY, USA), 50 μg/mL gentamicin (Mediatech), 150 μg/mL neomycin sulfate (Sigma, Inc., St. Louis, MO, USA), 1.5 μg/mL fungizone (Sigma), and 455 μg/mL streptomycin. Before virus inoculation, the cells were washed three times with Hanks' balanced salt solution (pH 7.3). After virus inoculation, the cells were kept at 37°C for 1 h for virus adsorption. Maintenance medium without FBS was used for propagation of TGEV. For SIV and AIV, the maintenance medium contained trypsin (1.5 μg/mL, Sigma) and 4% bovine serum albumin (BSA; Gibco, Life Technologies, Corp.). Inoculated cells were incubated at 37°C under 5% CO_2. After the appearance of virus-induced cytopathic effects (CPE),

usually at 4–5 days post-infection, the cells were subjected to three freeze-thaw cycles (−80°C/25°C) followed by centrifugation at 2500 × g for 15 min at 4°C. The supernatant was collected and aliquoted into 50 mL tubes followed by storage at −80°C until use. For titration of TGEV in virus stock and other samples, serial ten-fold dilutions were prepared in MEM. For titration of SIV and AIV, 4% BSA and trypsin were added to MEM. Sample dilutions were inoculated in appropriate cell monolayers in 96-well microtiter plates (Nunc, Inc., NY, USA) using 100 μL/well. Four wells were used per dilution. Inoculated cells were incubated at 37°C under 5% CO_2 for 4–5 days until the CPE appeared. Virus titers were calculated as $TCID_{50}$/mL by the Karber method (Karber 1931).

2.3. Quantification of Total Virus by qRT-PCR

Viral RNA was extracted from 140 μL of sample using the QIAamp viral RNA kit (Qiagen, Inc., Valencia, CA, USA). The RNA was eluted in 40 μL of elution buffer and stored at –20°C until used for qRT-PCR (quantitative real time-PCR). The copy number of viral RNA present in each sample was quantified by RT-PCR performed in a Mastercycler Realplex thermocycler (Eppendorf, Hamburg, Germany) using QIAGEN One Step RT-PCR kit (Qiagen). Forward primers, reverse primers, and probes have been described by O'Connell et al. (2006) and Spackman et al. (2002). Samples were loaded in a 96-well plate and analyzed in duplicate, each containing 3 μL of viral RNA template in a final volume of 20 μL. Standard curves were constructed using serial ten-fold dilution of viral RNA extracted from the virus stock of known titer. In each run of qRT-PCR, standard curve samples and no template control were used as positive and negative controls. The thermal cycling conditions for RT, RT inactivation, and PCR of the four viruses were the same: 50°C for 30 min and 95°C for 15 min. The thermal cycling parameters were as follows: 40 cycles of 95°C for 15 s and 55°C for 45 s for MS2; 40 cycles of 95°C for 15 s and 60°C for 45 s for TGEV; and 45 cycles of 94°C for 1 s and 60°C for 20 s for SIV and AIV. Final results were expressed as cycle threshold (Ct) values. After qRT-PCR was performed, the amplification efficiency was determined for each sample using the DART-PCR method to correct the raw Ct values (Peirson et al. 2003). The average amplification efficiency was 0.87, 0.85, 0.84, and 0.90 for MS2, TGEV, SIV, and AIV, respectively. The corrected Ct values were then used, along with the standard curve, to calculate the concentration of total virus (live and inactivated) and was expressed as projected $TCID_{50}$/mL.

2.4. Aerosol Test Tunnel and Experiment Procedure

Experiments were performed in a one-pass aerosol test tunnel located in a biosafety Level 2 laboratory (Figure 1). The vertical tunnel was 1.7 m long and 15 cm in diameter, enclosed by a negative pressure containment to minimize release of virus aerosol into surrounding environment. It has been used in a variety of virus aerosol studies (Kim et al. 2007; Appert et al. 2012). Virus aerosol was generated using a six-jet Collison nebulizer (BGI, Inc., Waltham, MA, USA) at a compressed air pressure of 10 psi. The nebulizer suspension consisted of 45 mL thawed virus stock, 0.1 mL antifoam Y-204 (Sigma), and 5 mL uranine dye (0.25 g/mL, Fluka, Buchs, Switzerland), which served as a fluorescent particle tracer (Appert et al. 2012). The use of uranine allowed particle losses in the test

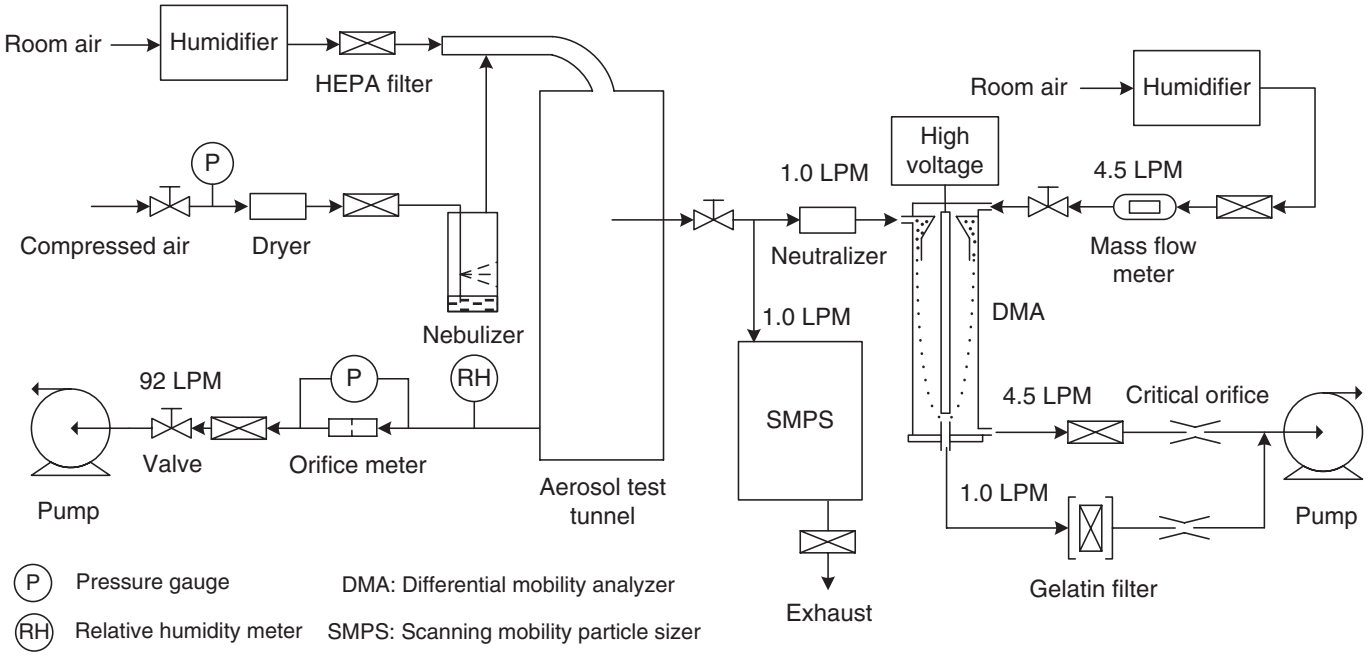

FIG. 1. Schematic diagram of the experimental setup for the characterization of virus aerosols.

system to be quantified. Virus titer in the freshly prepared nebulizer suspension was 3.1×10^9–5.8×10^9 PFU/mL (plaque forming unit per mL), 1.45×10^6–3.16×10^6 $TCID_{50}$/mL (50% tissue culture infectious dose per mL), 3.16×10^6–6.76×10^6 $TCID_{50}$/mL, and 3.16×10^5–1.48×10^6 $TCID_{50}$/mL for MS2, TGEV, SIV, and AIV, respectively.

The generated virus aerosol was mixed with HEPA-filtered and RH-controlled room air, and then directed to the test tunnel at a flow rate of 92 L/min. Two minutes were allowed for the produced virus aerosol to become well mixed and stabilized before samples were taken. Virus aerosol particles were passed through a polonium-210 neutralizer before being selected by a DMA (Model 3071; TSI, Inc., Shoreview, MN, USA) at 100, 200, 300, 400, and 450 nm. The sheath flow rate was 4.5 L/min, control by a critical orifice, and its RH was also controlled. The size-classified virus aerosol particles were collected onto 25 mm diameter gelatin filters with a pore size of 3 μm (SKC, Inc., Eight Four, PA, USA) held in a stainless steel holder (Millipore Corp., Bedford, MA, USA) at a sampling flow rate of 1 L/min for 15 min. Compared with the previously used liquid impinger (Hogan et al. 2005; Lee 2009), gelatin filters have excellent physical collection efficiency for virus aerosol particles (Burton et al. 2007) and do not significantly affect virus infectivity (Verreault et al. 2008) and were therefore used in this study.

The sampling time was limited to 15 min in order to minimize variation in the nebulizer output (Eninger et al. 2009) and desiccation of the collected virus. During the gelatin filter sampling, a scanning mobility particle sizer (SMPS) (Model 3034, TSI) was used to simultaneously measure the particle size distribution of the generated virus aerosol from 10 to 470 nm at a flow rate of 1 L/min. Immediately after sampling, the gelatin filter was removed from the filter holder, broken apart using sterile forceps, and dissolved in 1 mL of elution buffer (1.5% beef extract with 0.05 M glycine at pH of 7.2), followed by vortexing (American Scientific Products, Inc., McGaw Park, IL, USA) at maximal speed for 9–10 s, six times at 1 min intervals. The unsampled virus aerosol passed through the test tunnel and was finally filtered at the outlet. After each test, the nebulizer was turned off and the tunnel was purged for 15 min at 92 LPM using HEPA filtered clean air to remove any residual airborne particles.

In each test, 1 mL samples of nebulizer suspension before and after the test and 1 mL virus samples collected from the gelatin filter were split into three portions. The first portion was stored at 4°C until analyzed by a spectrofluorometer (Model RF-5201PC; Shimadzu Scientific Instruments, Inc., Columbia, MD, USA) to quantify the concentration of uranine in the sample (Appert et al. 2012). The results were expressed as fluorescence unit per mL. The latter two portions were stored at –80°C until virological analysis. Virus infectivity assay and quantitative reverse transcription-polymerase chain reaction (qRT-PCR) were used to quantify the amount of infectious and total (both infectious and non-infectious) virus present in the samples.

The tests were repeated in triplicate for MS2, TGEV, and SIV and twice for AIV. During the experiments, the RH and temperature in the test tunnel were maintained at 40–50% and 22–25°C, respectively.

2.5. Data Analysis

To determine the distribution of virus in polydisperse particles and compare it with particle size distribution, the infectious virus size distribution, $IV(D_p)$ was defined particularly for particles carrying infectious virus (Hogan et al. 2005) and calculated as:

$$IV(D_P) \equiv \frac{dC_{IV}(D_P)}{d\log_{10} D_P} \approx \frac{C_{IV,gel}(D_P)\, V_{gel}}{Q_{gel} t[\Delta \log_{10} D_P]} \frac{1}{f_{+1}(D_P)\, P(D_P)}, \quad [1]$$

where C_{IV} is the concentration of airborne infectious virus, $C_{IV,gel}$ is the concentration of infectious virus recovered in the effluent from the gelatin filter, V_{gel} is the volume of eluent used to dissolve the gelatin filter, Q_{gel} is the air sampling flow rate through the gelatin filter, t is the sampling time, $\Delta log_{10} D_p$ is the logarithm of the width of the size interval of the DMA, f_{+1} is the fraction of singly positively charged particles (Wiedensohler 1988), and P is penetration of particles through the DMA (Reineking and Porstendorfer 1986). Similarly, by replacing the concentration of infectious virus with that of total virus, the total virus size distribution, $TV(D_p)$ can be calculated as:

$$TV(D_P) \equiv \frac{dC_{TV}(D_P)}{d\log_{10} D_P} \approx \frac{C_{TV,gel}(D_P)\, V_{gel}}{Q_{gel} t[\Delta \log_{10} D_P]} \frac{1}{f_{+1}(D_P)\, P(D_P)}. \quad [2]$$

The amount of infectious virus carried per particle, iv, was calculated as the ratio of infectious virus concentration to particle number concentration, assuming the $\Delta log_{10} D_p$ interval is the same for the DMA and the SMPS:

$$iv(D_P) \equiv \frac{dC_{IV}(D_P)}{dC_{n,SMPS}(D_P)} \approx \frac{C_{IV,gel}(D_P)\, V_{gel}}{Q_{gel} t\, \Delta C_{n,SMPS}(D_P)} \frac{1}{f_{+1}(D_P)\, P(D_P)}, \quad [3]$$

where $\Delta C_{n,SMPS}$ is the number concentration of particles within a size interval with geometric diameter D_p measured by the SMPS. Similarly, the amount of total virus carried per particle, tv, was calculated as:

$$tv(D_P) \equiv \frac{dC_{TV}(D_P)}{dC_{n,SMPS}(D_P)} \approx \frac{C_{TV,gel}(D_P)\, V_{gel}}{Q_{gel} t\, \Delta C_{n,SMPS}(D_P)} \frac{1}{f_{+1}(D_P)\, P(D_P)}. \quad [4]$$

Power-law curve fitting with least squares was conducted for $iv(D_p)$ and $tv(D_p)$ using Microsoft Excel.

The effect of nebulization stress on virus infectivity and viral RNA integrity was also examined by calculating the terms γ_{IV} and γ_{TV} (Appert et al. 2012):

$$\gamma_{IV} = \frac{(C_{IV,neb}/C_{F,neb})_a}{(C_{IV,neb}/C_{F,neb})_b} \quad \gamma_{TV} = \frac{(C_{TV,neb}/C_{F,neb})_a}{(C_{TV,neb}/C_{F,neb})_b}, \qquad [5]$$

which compare the ratio of infectious virus ($C_{IV,\,neb}$) or total virus concentration ($C_{TV,\,neb}$) to fluorescence intensity ($C_{F,\,neb}$) in the nebulizer suspension before (b) and after (a) the nebulization. The fluorescence intensity was included in the calculation to take into account the increase of virus titer due to the evaporation of liquid from the nebulizer suspension.

To quantify how efficiently infectious virus could be recovered by the DMA and gelatin filter based sampling system, relative recovery of infectious virus, RR_{IV} was calculated as a function of particle size (Ijaz et al. 1987; Agranovski et al. 2005; Appert et al. 2012):

$$RR_{IV}(D_P) = \frac{C_{IV,gel}(D_P)/C_{F,gel}(D_P)}{C_{IV,neb}/C_{F,neb}}, \qquad [6]$$

where $C_{IV,neb}$ and $C_{F,neb}$ are the average of readings before and after tests.

Similarly, relative recovery of total virus, RR_{TV} was also calculated, to evaluate how efficiently viral RNA was recovered:

$$RR_{TV}(D_P) = \frac{C_{TV,gel}(D_P)/C_{F,gel}(D_P)}{C_{TV,neb}/C_{F,neb}}. \qquad [7]$$

Finally, the particle size dependent virus survivability, S, was determined by calculating the ratio of infectious virus to total (both infectious and non-infectious) virus carried by the particles normalized by the same ratio in the nebulizer suspension:

$$S(D_P) = \frac{C_{IV,gel}(D_P)/C_{TV,gel}(D_P)}{C_{IV,neb}/C_{TV,neb}}. \qquad [8]$$

Data were statistically analyzed using one-way or multiple-way analysis of variance (ANOVA) in Matlab (MathWorks, Inc., Natick, MA, USA). The limit of detection (LOD) of the Kaber method is 10 $TCID_{50}$/mL. For samples where no infectious virus was detected (two out of the three replicates of SIV at 100 nm), a value equal to LOD divided by square root of 2 was used in the calculation (Hornung and Reed 1990).

3. RESULTS

3.1. Size Distribution of Virus Aerosol Particles

As a first step to characterize the virus aerosols, the size distributions of the four virus aerosols were determined using the SMPS (Figure S1, available in the online supplementary information). The size distributions were generally lognormal with the statistics provided in Table S1. There was no clear correlation between the size of virion and the size of generated virus aerosol. Small virion size did not necessarily give a small count median diameter.

3.2. Infectious/Total Virus Size Distribution

Figure 2 and Figure S3 (available online only) represent the infectious virus and total virus size distribution from 100 nm to 450 nm normalized by the maximum values. In general, both the infectious and total virus concentrations increased with particle size and the maximum values at 400–450 nm were around 5000 PFU/cm^3, 35 $TCID_{50}$/cm^3, 180 $TCID_{50}$/cm^3, and 60 $TCID_{50}$/ cm^3 for MS2, TGEV, SIV, and AIV, respectively, which were several orders of magnitude lower than the particle number concentration at the same particle size. The virus size distributions were normalized to compare them more easily with particle size distributions. As seen in Figures 2 and S3, the infectious and total virus distributions had a similar trend, both appearing to follow particle volume distribution rather than particle number distribution. Infectious and total virus concentrations collected by the gelatin filters are available online (Table S2).

3.3. Infectious/Total Virus Carried Per Particle

The average amount of infectious virus and total virus carried by each particle (*iv* and *tv*) were plotted as a function of particle size (Figures 3 and S4). For all four viruses, *iv* and *tv* increased with particle size. The values were much lower than unity, even at 450 nm. Power-law curve fitting gave R^2-values ranging from 0.75 to 0.99, suggesting that there was a power-law correlation between *iv*/*tv* and particle size. Note that the slopes obtained

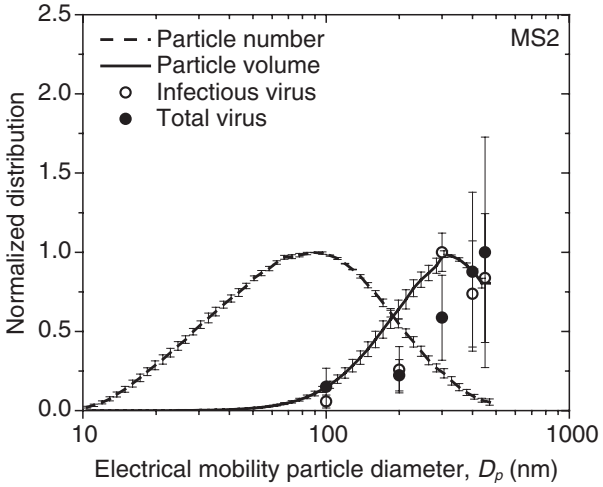

FIG. 2. Normalized infectious virus size distribution, total virus size distribution, SMPS particle number distribution, and SMPS particle volume distribution for airborne MS2. Values are means ± one standard deviation ($n = 3$). Similar plots for TGEV, SIV, and AIV are available online (Figure S3).

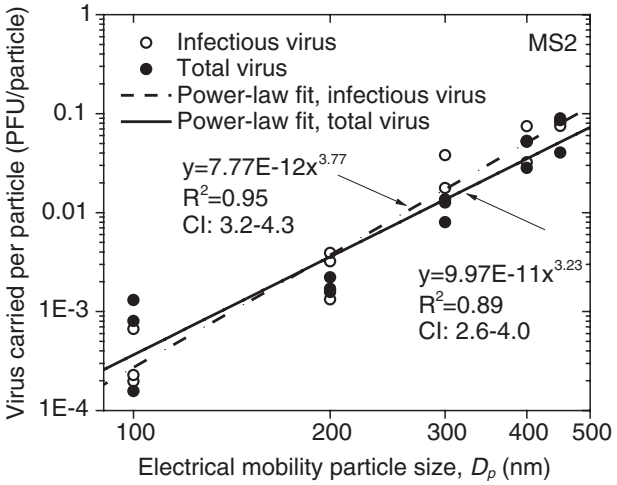

FIG. 3. Infectious virus and total virus carried per particle as a function of particle size for airborne MS2. Also shown are the equations and R^2-values of the curve fitting and the 95% confidence intervals (CI) of the slopes, where x represents the particle size and y represents the amount of either infectious virus or total virus carried per particle. Note that the slopes of the lines are the exponents of the equations. Similar plots for TGEV, SIV, and AIV are available online (Figure S4).

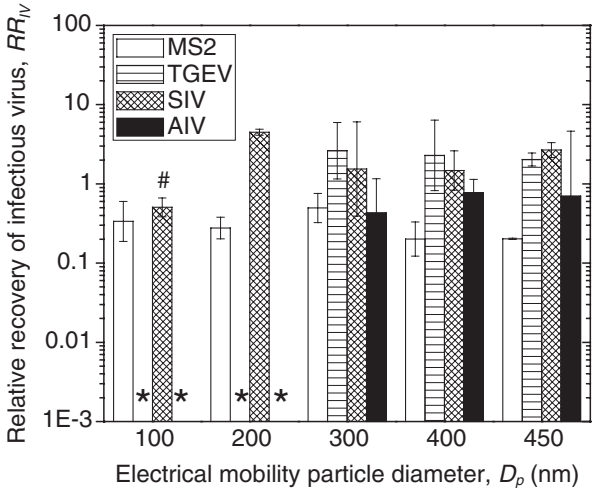

FIG. 4. Relative recovery of infectious virus. Each bar represents geometric mean ± one standard deviation of the mean. In cases where no infectious virus was recovered (denoted by asterisks [*]), an infectious virus concentration of 10 $TCID_{50}$/mL was used to estimate RR_{IV}, which was lower than 0.47, 0.07, 0.86, and 0.10 for TGEV at 100 and 200 nm and AIV at 100 and 200 nm, respectively. The pound sign (#) denotes that infectious virus was recovered in only one of the three samples.

from the curve fits were significantly greater than three in some cases.

3.4. Nebulization Stress on Virus

As shown in Figure S2, terms γ_{IV} and γ_{TV} were not significantly different from unity for the four viruses. In addition, neither γ_{IV} ($p = 0.276$) nor γ_{TV} ($p = 0.536$) were found to significantly depend on the type of virus using one-way ANOVA.

3.5. Relative Recovery of Infectious Virus and Total Virus

Figure 4 shows RR_{IV} as a function of particle size for the four viruses. For MS2, RR_{IV} was around 0.3, independent of particle size ($p = 0.245$, one-way ANOVA). However, for the three animal viruses, RR_{IV} showed strong particle size dependence with values at 100–200 nm much lower than those at 300–450 nm. At particle sizes of 300 nm and above, RR_{IV} became independent of particle size ($p = 0.948$, two-way ANOVA) but was significantly affected by the type of virus ($p = 0.001$, two-way ANOVA). RR_{IV} of TGEV and SIV were generally higher than MS2 and AIV at particle sizes 300 nm and above.

Contrary to RR_{IV}, RR_{TV} did not depend on particle size ($p = 0.954$, two-way ANOVA) for any of the four viruses (Figure 5). However, it was significantly affected by the type of virus ($P < 0.001$, two-way ANOVA). The particle size-averaged RR_{TV} was 1.05, 2.22, and 1.36 for TGEV, SIV, and AIV, respectively, much higher than MS2 (0.26).

3.6. Survivability of Airborne Viruses

Virus survivability was plotted as a function of particle size for the four viruses (Figure 6). Similar to RR_{IV}, the survivability of MS2 was roughly a constant, independent of particle size ($p = 0.397$, one-way ANOVA). However, the three animal viruses demonstrated enhanced survivability at 300–450 nm, compared with 200 nm. At large particle size (300–450 nm), virus survivability was found to be independent of particle size ($p = 0.912$, two-way ANOVA) and the particle size averaged survivability was 1.00, 1.86, 0.75, and 0.41 for MS2, TGEV,

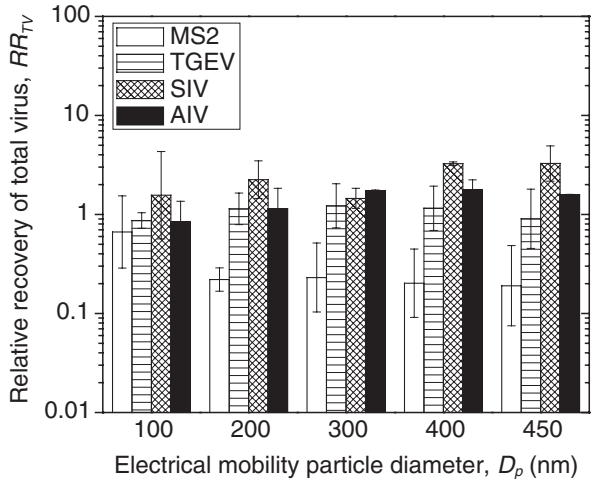

FIG. 5. Relative recovery of total virus. Each bar represents geometric mean ± one standard deviation of the mean.

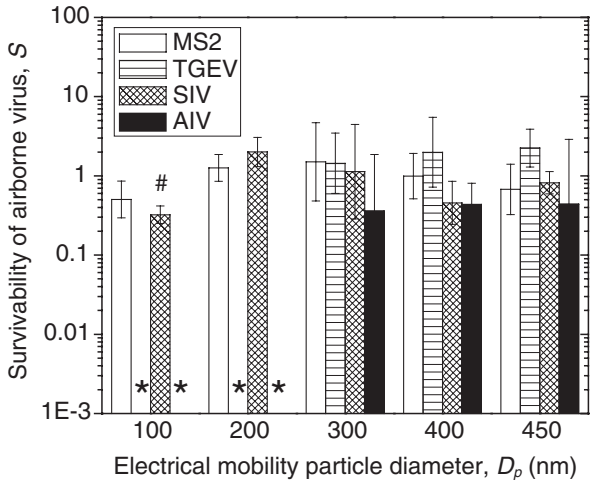

FIG. 6. Survivability of airborne virus. Each bar represents geometric mean ± one standard deviation of the mean. In cases where no infectious virus was recovered (denoted by asterisks [*]), an infectious virus concentration of 10 $TCID_{50}$/mL was used to estimate *S*, which was lower than 0.42, 0.06, 1.02, and 0.10 for TGEV at 100 and 200 nm and AIV at 100 and 200 nm, respectively. The pound sign (#) denotes that infectious virus was recovered in only one of the three samples.

SIV, and AIV, respectively, though the difference was not statistically significant ($p = 0.080$, two-way ANOVA).

4. DISCUSSION

4.1. Comparison Between Particle Size Distribution and Virus Size Distribution

Pneumatic nebulizers such as the Collison are commonly used in laboratory studies to produce virus aerosol from liquid suspensions (Reponen et al. 1997). However, the measured particle size distributions (Figure S1) showed that the traditional Collison nebulizer inevitably generated residue particles carrying no virus. For example, many particles were found at sizes smaller than the virion size. The mean particle size of MS2 virus aerosol was larger than other studies also using Collison nebulizers (Hogan et al. 2005 and Eninger et al. 2009), which could result from the much higher solute concentration (e.g., the addition of uranine) in the nebulizer suspension used in this study. Unlike the narrow size range of virions, the generated aerosol covered a much wider range (Table S1), suggesting that the nebulizer could generate high concentration of residue particles, due to the chemicals dissolved in the virus/cell growth media, which is consistent with the observations of Hogan et al. (2005).

Therefore, the particle number distribution, though easily measured by an SMPS, does not necessarily indicate how virus is distributed among particles of different sizes. In fact, the virus size distribution was indeed masked by the particle number distribution (Figures 2 and S3). Lee (2009) found that infectious virus size distribution for MS2 at 30–230 nm followed particle volume distribution. This study confirmed Lee's observation for MS2 and showed for the first time that both infectious virus and total virus distributions of the three respiratory viruses were much better represented by particle volume distribution than number distribution in the size range of 100–450 nm (Figure S3). Recently, there is a growing interest in evaluating filter performance using different particle size-integrated penetration measurements (Li et al. 2012). Based on the understanding of virus size distributions presented here, perhaps particle mass-based filter efficiency may better represent the performance of a filter against airborne virus, compared with particle number- or surface area-based efficiency.

4.2. Probability for a Particle to Carry Virus

As a further step to understand how virus infectivity depends on particle size, the amount of infectious virus (*iv*) and total virus (*tv*) carried per particle was determined as a function of particle size (Figures 3 and S4). Assuming one PFU represents one virion, the probability for a 450 nm particle to carry one MS2 virion was $<10\%$. The reported ratio of infectious virus per $TCID_{50}$ in particles ranged between 30 and 300 for influenza virus (Wei et al. 2007; Fabian et al. 2008). Using a similar ratio, the probability for a 450 nm nebulizer-generated particle to carry one animal virus was estimated to be $<100\%$. Therefore, the results suggest that only a small fraction of laboratory generated particles actually carry virus, even when a nebulization suspension of high virus titer is used and the particle size is larger than the virion. However, the capacity for a particle to carry virus increased with particle size, following a power law relationship. Interestingly, a slope of >3 was found in all the cases and some were even significantly greater than three, which indicated the amount of virus carried by a particle was proportional to more than the particle volume. This finding also agreed with the virus size distributions, which seemed to be shifted to larger sizes compared with the particle volume distributions (Figures 2 and S3). Multiple-charged particles of larger size (presumably carrying more virus) with the same electrical mobility could be collected by the gelatin filter, which may increase the slope. Nebulization suspension may also affect the slope. For example, Lee (2009) found that the slope changed from $\sim$3 for DI water to $\sim$2.5 for tryptone solution. In general, *iv* and *tv* depend on particle size, the type of virus, and the nebulizer suspension.

4.3. Effect of Aerosolization on Virus Infectivity and Viral RNA

Although high shear stress during aerosolization can reduce viability of bacteria (Griffiths and DeCosemo 1994), aerosolization for a short time period (2–30 min) has been shown to have a negligible effect on virus infectivity (Harper 1961; Ijaz et al. 1985; Appert et al. 2012). This study evaluated the effect of a longer aerosolization time ($\sim$90 min) on both virus infectivity and total virus (viral RNA). As shown in Figure S2, the values of γ_{IV} and γ_{TV} suggest that neither infectious

virus nor viral RNA was significantly affected by aerosolization. Fabian et al. (2009) also found that the ratio of total virus to infectious virus in the nebulizer suspension only slightly increased over an aerosolization time of 70 min. The four viruses had similar γ, indicating that aerosolization had a similar effect on each virus, independent of virion size and surface structure (e.g., naked or enveloped). The smaller size of virions compared with bacteria might explain the virus resistance to aerosolization stress (Kim et al. 2007). Viruses tend to form aggregates in liquid suspension (Hogan et al. 2004; Wei et al. 2007). However the continuous recirculation of virus suspension through the nebulizer nozzle may reduce the level of aggregation and thus increase virus titer (Teunis et al. 2005), which may also explain $\gamma_{IV} \approx 1$.

4.4. Relative Recovery of Infectious Virus and Total Virus

For TGEV and AIV, RR_{IV} at 200 nm was much lower compared with 300–450 nm (Figure 4). Because no infectious virus was detected at 100–200 nm, an infectious virus concentration of 10 $TCID_{50}$/mL was used to estimate RR_{IV}. Since 200 nm particles carried more fluorescence than those at 100 nm, the estimated RR_{IV} at 100 nm was much higher than 200 nm for TGEV and AIV. RR_{IV} is often used to evaluate how efficiently certain sampling systems can recover infectious virus aerosol shortly after its generation and theoretically $RR_{IV} \leq 1$ (Ijaz et al. 1987; Agranovski et al. 2005; Appert et al. 2012). However, $RR_{IV} > 1$ was sometimes found for TGEV and SIV, which could be due to the large uncertainty of animal virus titration. For example, a difference in one well of cell cytopathic change yields almost twice the difference in the final titration results.

If there is no loss of total virus (viral RNA), then $RR_{TV} = 1$, assuming the amount of virus carried by a particle is proportional to the particle volume and measurement errors are negligible. As demonstrated in Figure 5, the animal virus nucleic acids were generally recovered without loss, suggesting they were as stable as the fluorescence tracer. Therefore, for the three animal viruses tested, their viral RNAs could potentially be used as an alternative to traditional chemical tracers such as uranine, though their lower detection limit (Verreault et al. 2008) and long time stability should be further tested.

4.5. Survivability of Airborne Virus

Similar to RR_{IV}, survivability of TGEV and AIV was much lower at 200 nm than at larger size (Figure 6). One could argue that the discretization phenomenon is responsible for this finding, i.e., as the carrier particle size gets smaller and approaches the size of virion, it becomes more difficult for the particle to carry virus. However, the particle size-independent RR_{TV} shown in Figure 5 suggests the presence of virus in particles even at 100 nm. Therefore, the discretization phenomenon was probably not the reason. The main reason for the particle size associated survivability could be the shielding effect. More specifically, compared with virus existing as a singlet or in association with fewer organics (e.g., solutes in the nebulizer suspension), the virus at larger particles may be surrounded by more organic material, which may form a shield. Shielding effect has been demonstrated to better protect virus from environmental stress such as ultraviolet irradiation (Woo et al. 2012). It may also reduce sampling stress such as desiccation and sampler dependent-mechanical forces, thus better maintaining the infectivity of airborne virus. However, as particle size increased to 300 nm and above, virus survivability seemed to reach a plateau, suggesting the shielding effect was maintained once a specific particle size was reached. The same explanation applies to MS2. Because all collected particle sizes were more than four times the virion size (27–34 nm), the survivability reached the plateau regime and therefore was no longer depended on particle size (Figure 6). This is supported by Lee (2009), who showed that survivability of MS2 at 120–200 nm was higher than at 30 nm, despite the large experimental variation.

Any loss of airborne virus survivability must eventually result from inactivation of the outer virus protein coat and/or inner nucleic acid core (Sattar and Ijaz 1987). Figures 4–6 suggest that MS2 was inactivated mainly due to the damage of its viral RNA. For MS2 with intact viral RNA, its infectivity was well maintained with survivability of $\sim$1. Because aerosolization has been shown to have minimal effect on the virus (Figure S2) and exposing MS2 collected on gelatin filters to an air stream for 10 min did not affect virus infectivity (Grinshpun et al. 2007), we believe that the loss of MS2 virus infectivity and viral RNA mostly occurred in the aerosol phase. Since, the animal viruses generally had intact viral RNAs ($RR_{TV} \approx 1$), their inactivation was probably due to the damage of the virus envelope and/or capsid. Inactivation of picornavirus and poliovirus, both non-enveloped viruses, has been shown to result from denaturation of the virus protein coat and viral nucleic acid, respectively (Akers and Hatch 1968; De Jong and Winkler 1968).

In general, MS2 and TGEV survived best, followed by SIV and AIV. Unfortunately, without additional tests (e.g., exposing viruses collected on gelatin filters to air streams and determining infectivity loss), we could not determine if the inactivation of animal viruses happened during the aerosol phase, sampling phase, or both. Note that SIV showed high survivability at 200 nm compared with AIV (Figure 6), suggesting influenza virus of different subtypes may have different survivability, which confirms the findings in other studies (Schaffer et al. 1976; Pyankov et al. 2012).

4.6. Use of MS2 Bacteriophage as a Surrogate Virus

Several advantages such as non-pathogenicity, high virus titer, and simple infectivity assay make MS2 bacteriophage widely used in virus aerosol studies. However, similar to a previous study (Appert et al. 2012), its different recovery and infectivity/survivability compared with corona and influenza virus suggests that it may not be a suitable general surrogate for animal or human viruses. Using surrogates that over-/underestimate the

inactivation of the target microorganisms may negatively impact risk assessment (Sinclair et al. 2012).

4.7. Limitations

One of the limitations of this study was that the virus was aerosolized from its stock suspension, which is unlikely to represent the liquid surrounding airborne viruses when they are generated from infected animals or humans. In addition, it is not clear if the generation mechanism of human expiratory particles is the same as the Collison nebulizer. Therefore, one should be cautious in generalizing the experimental results to real life situations since infectivity and survivability of airborne virus may heavily depend on the composition of the nebulizer suspension (Sattar and Ijaz 1987) and the way it is generated.

5. CONCLUSIONS

In conclusion, we systematically measured virus concentration, virus survivability, and particle concentration as a function of particle size using four different viral aerosols. The DMA and gelatin filter based sampling system combined with virus infectivity assay and qRT-PCR analysis is a useful way to characterize laboratory generated virus aerosol in the submicron size range with high size resolution. Our results demonstrate that particle size has a significant effect on infectivity and survivability of airborne virus, which emphasizes the importance of particle size in the transmission of viral diseases by the aerosol route. Different behavior of MS2 bacteriphage compared with TGEV, SIV, and AIV calls into question its use as a general surrogate for animal and human viruses. Methods and results presented here may be utilized in various studies to help better understand and control the airborne transmission of virus.

REFERENCES

Agranovski, I., Safatov, A., Pyankov, O., Sergeev, A., and Grinshpun, S. A. (2005). Long-Term Sampling of Viable Airborne Viruses. *Aerosol Sci. Technol.*, 39:912–918.

Akers, T. G., and Hatch, M. T. (1968). Survival of a Picornavirus and Its Infectious Ribonucleic Acid After Aerosolization. *Appl. Microbiol.*, 16:1811–1813.

Alford, R. H., Kasel, J. A., Gerone, P. J., and Knight, V. (1966). Human Influenza Resulting from Aerosol Inhalation. *Proc. Soc. Exp. Biol. Med.*, 122:800–804.

Appert, J., Raynor, P. C., Abin, M., Chander, Y., Guarino, H., Goyal, S. M., et al. (2012). Influence of Suspending Liquid, Impactor Type, and Substrate on Size-Selective Sampling of MS2 and Adenovirus Aerosols. *Aerosol Sci. Technol.*, 46:249–257.

Burton, N. C., Grinshpun, S. A., and Reponen, T. (2007). Physical Collection Efficiency of Filter Materials for Bacteria and Viruses. *Ann. Occup. Hyg.*, 51:143–151.

De Jong, J. C., and Winkler, K. C. (1968). The Inactivation of Poliovirus in Aerosols. *J. Hyg.*, 66:557–565.

Douglas, R. G. (1975). *Influenza in Man. The Influenza Viruses and Influenza*, E. D. Kilbourne, ed., Academic Press, New York.

Eninger, R. M., Honda, T., Adhikari, A., Heinonen-Tanski, H., Reponen, T., and Grinshpun, S. A. (2008). Filter Performance of N99 and N95 Facepiece Respirators Against Viruses and Ultrafine Particles. *Ann. Occup. Hyg.*, 52:385–396.

Eninger, R. M., Hogan, C. J., Biswas, P., Adhikari, A., Reponen, T., and Grinshpun, S. A. (2009). Electrospray Versus Nebulization for Aerosolization and Filter Testing with Bacteriophage Particles. *Aerosol Sci. Technol.*, 43:298–304.

Fabian, P., McDevitt, J. J., DeHaan, W. H., Fung, R. O. P., Cowling, B. J., Chan, K. H., et al. (2008). Influenza Virus in Human Exhaled Breath: An Observational Study. *PloS one*, 3:e2691. DOI: 10.1371/journal.pone.0002691.

Fabian, P., McDevitt, J. J., Houseman, E. A, and Milton, D. K. (2009). Airborne Influenza Virus Detection with Four Aerosol Samplers Using Molecular and Infectivity Assays: Considerations for a New Infectious Virus Aerosol Sampler. *Indoor Air*, 19:433–41.

Gerone, P. J., Couch, R. B., Keefer, G. V., Douglas, R. G., Derrenbacher, E. B., and Knight, V. (1966). Assessment of Experimental and Natural Viral Aerosols. *Bacteriol. Rev.*, 30:576–588.

Gralton, J., Tovey, E., McLaws, M. L., and Rawlinson, W. D. (2011). The Role of Particle Size in Aerosolised Pathogen Transmission: A Review. *J. Infect.*, 62:1–13.

Griffiths, W. D., and DeCosemo, G. A. L. (1994). The Assessment of Bioaerosols: A Critical Review. *J. Aerosol Sci.*, 25:1425–1458.

Grinshpun, S. A., Adhikari, A., Honda, T., Kim, K. Y., Toivola, M., Rao, K. S. R., et al. (2007). Control of Aerosol Contaminants in Indoor Air: Combining the Particle Concentration Reduction with Microbial Inactivation. *Environ. Sci. Technol.*, 41:606–612.

Hamory, B. H., Couch, R. B., Douglas, R. G., Black, H., and Knight, V. (1972). Characterization of the Infectious Unit for Man of Two Respiratory Viruses. *Proc. Soc. Exp. Biol. Med.*, 139:890–893.

Harper, G. J. (1961). Airborne Micro-Organisms: Survival Tests with Four Viruses. *J. Hyg.*, 59:479–486.

Haslbeck, K., Schwarz, K., Hohlfeld, J. M., Seume, J. R., and Koch, W. (2010). Submicron Droplet Formation in the Human Lung. *J. Aerosol Sci.*, 41:429–438.

Hemmes, J. H., Winkler, K. C., and Kool, S. M. (1960). Virus Survival as a Seasonal Factor in Influenza and Poliomyelitis. *Nature*, 188:430–431.

Hogan, C., Lee, M.-H., and Biswas, P. (2004). Capture of Viral Particles in Soft X-Ray-Enhanced Corona Systems: Charge Distribution and Transport Characteristics. *Aerosol Sci. Technol.*, 38:475–486.

Hogan, C. J., Kettleson, E. M., Lee, M.-H., Ramaswami, B., Angenent, L. T., and Biswas, P. (2005). Sampling Methodologies and Dosage Assessment Techniques for Submicrometre and Ultrafine Virus Aerosol Particles. *J. Appl. Microbiol.*, 99:1422–1434.

Holmgren, H., Ljungström, E., Almstrand, A.-C., Bake, B., and Olin, A.-C. (2010). Size Distribution of Exhaled Particles in the Range from 0.01 to 2.0 μm. *J. Aerosol Sci.*, 41:439–446.

Hornung, R. W., and Reed, L. D. (1990). Estimation of Average Concentration in the Presence of Nondetectable Values. *Appl. Occup. Environ. Hyg.*, 5:46–51.

Ijaz, M. K., Brunner, A. H., Sattar, S. A, Nair, R. C., and Johnson-Lussenburg, C. M. (1985). Survival Characteristics of Airborne Human Coronavirus 229E. *J. Gen. Virol.*, 66:2743–2748.

Ijaz, M. K., Karim, Y. G., Sattar, S. A., and Johnson-Lussenburg, C. M. (1987). Development of Methods to Study the Survival of Airborne Viruses. *J. Virol. Methods*, 18:87–106.

Jackwood, M. W. (2006). The Relationship of Severe Acute Respiratory Syndrome Coronavirus with Avian and Other Coronaviruses. *Avian Dis.*, 50:315–320.

Karber, G. (1931). Fifty Percent Endpoint Calculation. *Arch. Exp. Path. Pharmak.*, 162:480–487.

Kim, S. W., Ramakrishnan, M. A., Raynor, P. C., and Goyal, S. M. (2007). Effects of Humidity and Other Factors on the Generation and Sampling of a Coronavirus Aerosol. *Aerobiologia*, 23:239–248.

Lamb, R. A., and Choppin, P. W. (1983). The Gene Structure and Replication of Influenza Virus. *Ann. Rev. Biochem.*, 52:467–506.

Lee, J. H. (2009). *Assessment of the Performance of Iodine-Treated Biocidal Filters and Characterization of Virus Aerosols*. Ph.D. Thesis, University of Florida, Gainesville, FL.

Li, L., Zuo, Z., Japuntich, D. A., and Pui, D. Y. H. (2012). Evaluation of Filter Media for Particle Number, Surface Area and Mass Penetrations. *Ann. Occup. Hyg.*, 56:581–594.

Morawska, L. (2006). Droplet Fate in Indoor Environments, or Can We Prevent the Spread of Infection? *Indoor Air*, 16:335–347.

O'Connell, P. K., Bucher, R. J., Anderson, E. P., Cao, J. C., Khan, S. A., Gostomski, V. M., et al. (2006). Real-Time Fluorogenic Reverse Transcription-PCR Assays for Detection of Bacteriophage MS2. *Appl. Environ. Microbiol.*, 72:478–483.

Peirson, S. N., Butler, J. N., and Foster, R. G. (2003). Experimental Validation of Novel and Conventional Approaches to Quantitative Real-Time PCR Data Analysis. *Nucleic Acids Res.*, 31:73e–73e.

Pyankov, O. V., Pyankova, O. G., and Agranovski, I. E. (2012). Inactivation of Airborne Influenza Virus in the Ambient Air. *J. Aerosol Sci.*, 53:21–28.

Reineking, A., and Porstendörfer, J. (1986). Measurements of Particle Loss Functions in a Differential Mobility Analyzer (TSI, Model 3071) for Different Flow Rates. *Aerosol Sci. Technol.*, 5:483–486.

Reponen, T., Willeke, K., Ulevicius, V., Grinshpun, S. A., and Donnelly, J. (1997). Techniques for Dispersion of Microorganisms into Air. *Aerosol Sci. Technol.*, 27:405–421.

Sattar, S., and Ijaz, M. K. (1987). Spread of Viral Infections by Aerosols. *Crit. Rev. Environ. Sci. Technol.*, 17:89–131.

Schaffer, F. L., Soergel, M. E., and Straube, D. C. (1976). Survival of Airborne Influenza Virus: Effects of Propagating Host, Relative Humidity, and Composition of Spray Fluids. *Archiv. Virol.*, 273:263–273.

Scott, G. H., and Sydiskis, R. J. (1976). Responses of Mice Immunized with Influenza Virus by Aerosol and Parenteral Routes. *Infect. Immunity*, 13:696–703.

Sinclair, R. G., Rose, J. B., Hashsham, S. A., Gerba, C. P., and Haas, C. N. (2012). Criteria for Selection of Surrogates Used to Study the Fate and Control of Pathogens in the Environment. *Appl. Environ. Microbiol.*, 78:1969–1977.

Spackman, E., Senne, A. D., Myers, J. T., Bulaga, L. L., Garber, P. L., Perdue, L. M., et al. (2002). Development of a Real-Time Reverse Transcriptase PCR Assay for Type A Influenza Virus and the Avian H5 and H7 Hemagglutinin Subtypes. *J. Clin. Microbiol.* 40:3256–3260.

Tajima, M. (1970). Morphology of Transmissible Gastroenteritis Virus of Pigs. *Archiv. Virol.*, 29:105–108.

Tellier, R. (2009). Aerosol Transmission of Influenza A Virus: A Review of New Studies. *J. R. Soc. Interface*, 6:S783–S790.

Teunis, P. F. M., Lodder, W. J., Heisterkamp, S. H., and Roda Husman, A. M. (2005). Mixed Plaques Statistical Evidence How Plaque Assays May Underestimate Virus Concentrations. *Water Res.*, 39:4240–4250.

Tyrrell, D. A. J. (1967). The Spread of Viruses of the Respiratory Tract by the Airborne Route, *Symp. Soc. Gen. Microbiol.*, 17:286–306.

Valegard, K., Liljas, L., Fridborg, K., and Unge, T. (1990). The Three-Dimensional Structure of the Bacterial Virus MS2. *Nature*, 345:36–41.

Verreault, D., Moineau, S., and Duchaine, C. (2008). Methods for Sampling of Airborne Viruses. *Microbiol. Mol. Biol. Rev.*, 72:413–444.

Wei, Z., McEvoy, M., Razinkov, V., Polozova, A., Li, E., Casas-Finet, J., et al. (2007). Biophysical Characterization of Influenza Virus Subpopulations Using Field Flow Fractionation and Multiangle Light Scattering: Correlation of Particle Counts, Size Distribution and Infectivity. *J. Virol. Methods*, 144:122–132.

Wiedensohler, A. (1988). An Approximation of the Bipolar Charge Distribution for Particles in the Submicron Size Range. *J. Aerosol Sci.*, 19:387–389.

Woo, M. H., Grippin, A., Anwar, D., Smith, T., Wu, C. Y., and Wander, J. D. (2012). Effects of Relative Humidity and Spraying Medium on UV Decontamination of Filters Loaded with Viral Aerosols. *Appl. Environ Microbiol.*, 78:5781–5787.

Zuo, Z., Kuehn, T. H., and Pui, D. Y. H. (2012). Performance Evaluation of Filtering Facepiece Respirators Using Virus Aerosols. *Am. J. Infect. Control*, in press. DOI: 10.1016/j.ajic.2012.01.010.